Enhanced electrochemical sensing performance by In Situ electrocopolymerization of pyrrole and thiophene-grafted chitosan

Mehmet Senel, Muamer Dervisevic, Lars Esser, Esma Dervisevic, Jennifer Dyson, Christopher D. Easton, Victor J. Cadarso, Nicolas H. Voelcker

PII: S0141-8130(19)38274-1

DOI: https://doi.org/10.1016/j.ijbiomac.2019.12.013

Reference: BIOMAC 14040

To appear in: *International Journal of Biological Macromolecules*

Received date: 13 October 2019

Revised date: 25 November 2019

Accepted date: 2 December 2019

Please cite this article as: M. Senel, M. Dervisevic, L. Esser, et al., Enhanced electrochemical sensing performance by In Situ electrocopolymerization of pyrrole and thiophene-grafted chitosan, *International Journal of Biological Macromolecules*(2019), https://doi.org/10.1016/j.ijbiomac.2019.12.013

Enhanced Electrochemical Sensing Performance by *In Situ* Electrocopolymerization of Pyrrole and Thiophene-Grafted Chitosan

Mehmet Senel [a]*, Muamer Dervisevic [b,c], Lars Esser [c], Esma Dervisevic [d], Jennifer Dyson [e,f], Christopher D. Easton [c], Victor J. Cadarso [d,g] and Nicolas H. Voelcker [b,c,e,g,h] *

[a] Department of Pharmaceutical Sciences, University of California, Irvine, CA 92697-4625, United States.

[b] Monash Institute of Pharmaceutical Sciences, Monash University, Parkville, VIC 3052, Australia.

[c] Commonwealth Scientific and Industrial Research Organization (CSIRO) Manufacturing, Clayton, VIC 3168, Australia.

[d] Department of Mechanical and Aerospace Engineering, Monash University, Clayton, VIC 3800, Australia.

[e] Monash Institute of Medical Engineering (MIME), Monash University, Clayton, VIC 3800, Australia.

[f] Department of Biochemistry & Molecular Biology, Biomedicine Discovery Institute, Clayton, VIC, 3800, Australia.

[g] Victorian Node of the Australian National Fabrication Facility, Melbourne Centre for Nanofabrication (MCN), Clayton, Victoria 3168, Australia.

[h] Department of Materials Science and Engineering, Monash University, Clayton, VIC 3800, Australia.

*Corresponding authors;

Mehmet Senel

Department of Pharmaceutical Sciences, University of California, Irvine, CA 92697-4625, United States, E-mail: msenel@uci.com, msenel81@gmail.com

Nicolas H. Voelcker

Monash Institute of Pharmaceutical Sciences, Monash University, Parkville, VIC 3052, Australia, E-mail: nicolas.voelcker@monash.edu

Abstract

Nowadays, there is increasing number of electrochemical biosensors which utilize chitosan (Ch); as an enzyme immobilization matrix, and conductive nanomaterials; as electron carriers improving sensitivity of the biosensor. However, the challenge these sensors face is the lack of uniform dispersion of nanomaterials throughout the Ch film, which can negatively affect analytical performance of the biosensor. In this study, we report the development of an enzyme immobilization matrix that displays enhanced electrochemical performance thanks to a novel conductive thin film prepared via *in situ* electrocopolymerization of pyrrole (Py) and thiophene-grafted chitosan (Th-Ch). This is a simple thin film preparation method that can help overcome aforementioned challenges by providing a uniformly distributed conductive layer on the electrode. We are also for the first time reporting the synthesis and characterization of Th-Ch, where grafted Th plays an essential role as a linking group between Ch and Py. The resulting conductive Ch-based thin film was modified with glucose oxidase (GOx) which served as a model enzyme. *In situ* electrocopolymerization of Py with Th-Ch resulted in a highly conductive thin film enabling approximately 40% higher sensitivity when compared to a Py-Ch composite. This new type of composite thin film is promising in biosensor technology due to its biocompatibility, the chemically and physically modifiable structure, as well as its electrical conductivity.

***Keywords*:** conductive polymer, chitosan, *in situ* electrocopolymerization, thiophene, pyrrole, glucose biosensor

1. Introduction

Chitosan is obtained through the deacetylation of chitin, a material naturally present in crabs, shrimps, squid pens, and other shellfish [1]. This aminopolysaccharide is inexpensive, biodegradable, has antimicrobial activity, and most importantly, it is biocompatible [2]. The chemical structure of Ch is also very attractive as the intrinsic oxygen and nitrogen-based functional groups enable covalent modifications or ionic interaction-based cross-linking that could result in the formation of hydrogel-like deposits [3]. These properties have made Ch one of the most favorable materials in the biomedical research like biosensing, and in pharmaceutical formulations for the improvement of drug delivery [4].

Although Ch is electrically insulating, it has been widely used in the preparation of electrochemical biosensors as an immobilization matrix. This matrix is crucial for the fixation and maintenance of the 3D structure, and therefore activity of enzymes or other biomacromolecules while a biosensor is being prepared, optimized, and utilized. To overcome the issue of Ch not being conductive and to benefit from all of its desirable properties in electrochemical sensing, researchers have incorporated various electrically conductive nanomaterials into it. Those included carbon-based nanomaterials such as carbon nanotubes, carbon dots, graphene, etc., [5-7] as well as nanoparticles such as Au, Fe_3O_4, CuO, $NiFe_2O_4$, CdTe, ZnO, etc. [8-14]. However, obtaining uniform dispersions of nanomaterials throughout a Ch film remains a challenge yet to be resolved affecting the stability of biosensor and reproducibility of biosensor`s analytical behavior [15]. To overcome this challenge, electropolymerization of monomers in the presence of Ch and other nanomaterials has been attempted to obtain a conductive and uniform thin film layer on an electrode surface [8, 16-19]. This type of surface then allows the controlled assembly of biorecognition elements including enzymes [16]. Electropolymerization of various

conductive polymers such as poly(aniline) [20-22], poly(thiophene) (PTh) [23-25], and poly(pyrrole) (PPy) [17, 26, 27] have been used for the preparation of different biosensors with good analytical performances. Interestingly, thin films obtained by electrochemical copolymerization of two monomers such as Py and Th, demonstrated higher electrical conductivity when compared to the film of the respective homopolymers [28-30]. Therefore, we posited that combining Ch with conductive polymers in electrochemically-deposited thin films would result in improved biosensing performance and can surpass the performance of other Ch-based bionanocomposite sensing platforms.

In this work, the synthesis and characterization of new Th-Ch, the *in situ* electrocopolymerization of this Ch derivative together with Py, and the implementation of the new thin film for the construction of an amperometric glucose biosensor are reported. While incorporated Th branches link Ch and Py during electropolymerization, Th-Ch facilitated an-easy-to-prepare and efficient matrix for glucose oxidase enzyme (GOx) immobilization. Because of relatively low Th density within the Th-Ch polymer, Py was essential to use electropolymerization technique for the thin film preparation. Th density within Th-Ch polymer affect the hydrophobicity and thus substrate diffusion throughout the thin film, and therefore require to be at an optimum level for enzymatic biosensors. The effect of Th presence within Ch on the performance of the biosensor was studied with different combinations of Th, Ch, and Py. Results show that Th-Ch electropolymerized with Py facilitated the formation of a highly conductive thin film. Furthermore, the reported electrode modification method provides the ability to both entrap enzyme *during* electrocopolymerization, or immobilize it using surface chemistry *after* the electrocopolymerization. GOx was used as the model recognition element for the investigation of sensing performance of two aforementioned electrode modification methods.

This new Ch-PTh-PPy thin film is highly promising for the electrochemical sensing technology due to the ability to obtain uniform electrode surface coatings in a short time.

2. Methods and Materials

2.1. Materials

Glucose oxidase from Aspergillus Niger, chitosan, pyrrole, potassium hexacyanoferrate (III), potassium hexacyanoferrate (II) trihydrate, sodium chloride (NaCl), sodium p-toluenesulfonate, 1-ethyl-3-(3-dimethyllaminopropyl) carbodiimide hydrochloride (EDC), 2-(thiophene-3-yl) acetic acid (Th-AA), and glutaraldehyde were purchased from Sigma Aldrich Chemical Co. All chemicals were of analytical grade and used without further purification.

2.2. Instrumentation

Electrochemical measurements were carried out using a CHI Mode 842B analyzer (CH Instruments Inc.) potentiostat with a conventional three electrodes electrochemical cell equipped with Ag/AgCl reference electrode (CH Instrument), pencil graphite electrode (PGE) working, and Pt wire counter electrodes. Error bars represent standard deviation (SD) of data set obtained from the measurements of separate three electrodes (n=3). Proton nuclear magnetic resonance (^{1}H NMR) analysis of Ch and Th-functionalized Ch were performed in deuterium water (D_2O) containing 5% deuterated acetic acid (CD_3COOD) using a Bruker Av 400 NMR spectrometer. Data processing was performed using MestReNova v6. Attenuated total reflection-Fourier transform infrared (ATR-FTIR) analysis of the materials was performed with a Thermo Scientific Nicolet 6700 FT-IR. The samples were dried in vacuum for overnight before the measurement (each 64 scans). Thermogravimetric analysis (TGA) was carried out using a Mettler Toledo TGA2. First, the sample was kept at 25°C for 30 min

under nitrogen flow (10 mL/min) then the temperature was increased to 700°C (again under nitrogen flow, 10°C/min). A Bruker FastScan atomic force microscope (AFM) with Icon scanning head and NanoScope 9.4 software was used to measure surface topography in ScanAsyst mode. Ultra-sharp silicon nitride tips were used for imaging under ambient (ScanAsyst-Air, Bruker Corporation) conditions. The tips had a typical force constant of 0.4 N/m and a resonant frequency of 70 kHz. A region of 1 μm was scanned at 0.7 Hz and 512 data points per scan line. The peak-force set point, while controlled by the instrument, was typically less than 2 nN. All images were processed, and lines scans obtained using NanoScope Analysis 1.9 software. X-ray photoelectron spectroscopy (XPS) analysis was performed using an AXIS Nova spectrometer (Kratos Analytical Inc., Manchester, UK) with a monochromated Al K_α source at a power of 180 W (15 kV × 12 mA) and a hemispherical analyzer operating in the fixed analyzer transmission mode. The total pressure in the main vacuum chamber during analysis was typically between 10^{-9} and 10^{-8} mbar. Survey spectra were acquired at pass energy of 160 eV. To obtain more detailed information about chemical structure and oxidation states, high-resolution spectra were recorded from individual peaks at 40 eV (yielding a typical peak width for polymers of 1.0 eV). Each specimen was analyzed at an emission angle of 0° as measured from the surface normal. Assuming typical values for the electron attenuation length of relevant photoelectrons, the XPS analysis depth (from which 95% of the detected signal originates) ranges between 5 and 10 nm for a flat surface. Data processing was performed using CasaXPS processing software version 2.3.15 (Casa Software Ltd., Teignmouth, UK). All elements present were identified from survey spectra. The atomic concentrations of the detected elements were calculated using integral peak intensities and the sensitivity factors supplied by the manufacturer. Binding energies were referenced to the C 1s peak at 285.0 eV. The accuracy associated with quantitative XPS is ca. 10-15%. Precision (i.e., reproducibility) depends on the signal/ noise ratio but is usually

lower than 5%. The latter is relevant when comparing similar samples. Scanning electron microscopy (SEM) imaging was carried out using a Hitachi TM3030 SEM.

2.3. Synthesis of thiophene-grafted chitosan (Th-Ch)

The Th-Ch was prepared by the formation of amide linkages through an EDC-mediated reaction following a similar method reported before [18]. 1 g of Ch was dissolved in 100 mL acetic acid solution (1% w/v) and diluted with 85 mL of methanol. Th-AA was added to this Ch solution at 0.54 mole:mole ratio glucosamine residue of chitosan followed by a dropwise addition of 15 mL of methanolic solution of EDC (0.07 g/L) while stirring at room temperature (RT). EDC and Th-AA had 1 to 1 mole ratio in this process. After 24 h, the reaction mixture was poured into 200 mL of methanol/ammonia solution (7/3, v/v) while being continuously stirred. The crude product was filtered, washed with distilled water (dH_2O), methanol and ether, and then dried under vacuum for 24 h at RT.

2.4. *In situ* electrocopolymerization and the fabrication of the biosensor

Biosensor fabrication was performed according to the procedure illustrated in Fig. 1. Prior to electrocopolymerization, all impurities and adsorbed organic material were removed from the surface of PGE with sonication performed in ethanol for 3 min. Then the PGE was rinsed with dH_2O and dried at RT. After the cleaning process, 7.5 µL of 1% (w/v) Th-Ch solution prepared in 1% (v/v) aqueous solution of acetic acid was drop-casted on the PGE surface and left to dry at RT. Then, the Th-Ch electrode was dipped into 1 M Py solution prepared using a 10 mM NaCl buffer containing 10 mM sodium-p-toluenesulfonate for 10 min. During this time, the Th-Ch layer swelled and absorbed the Py solution together with NaCl buffer and sodium-p-toluenesulfonate. Afterwards, *in situ* electrocopolymerization process was carried out using cyclic voltammetry (CV) with an applied potential range of 0.0

V to 1.0 V at 100 mV/s scan rate in 10 mM NaCl buffer containing 10 mM sodium-p-toluenesulfonate (the resulting thin film is termed Ch-PTh-PPy).

Two enzyme immobilization strategies were used for surface functionalization of the electrode. The first method involved the enzyme immobilization onto Ch-PTh-PPy where the electrode was immersed in 2.5% (v/v) aqueous solution of glutaraldehyde for 45 min, then washedwith dH_2O for several times, and then immersed in 15 mg/mL GOx solution for 2 h at 4°C (the resulting working electrode was named as Ch-PTh-PPy/GOx). The second method involved the entrapment of GOx into the Ch-PTh-PPy layer. It was carried out by dropping a mixture of 15 mg/ml of GOx and Th-Ch onto the bare PGE surface and drying the electrode at RT. Later, the electrode was immersed in the Py solution, and then electropolymerization was carried out as described above (the resulting electrode was named as Ch-PTh-GOx-PPy). To compare Th-Ch and Ch alone, the same protocols were used in the preparation of Ch-based electrodes. The working electrodes were stored at 4ºC when not being in use.

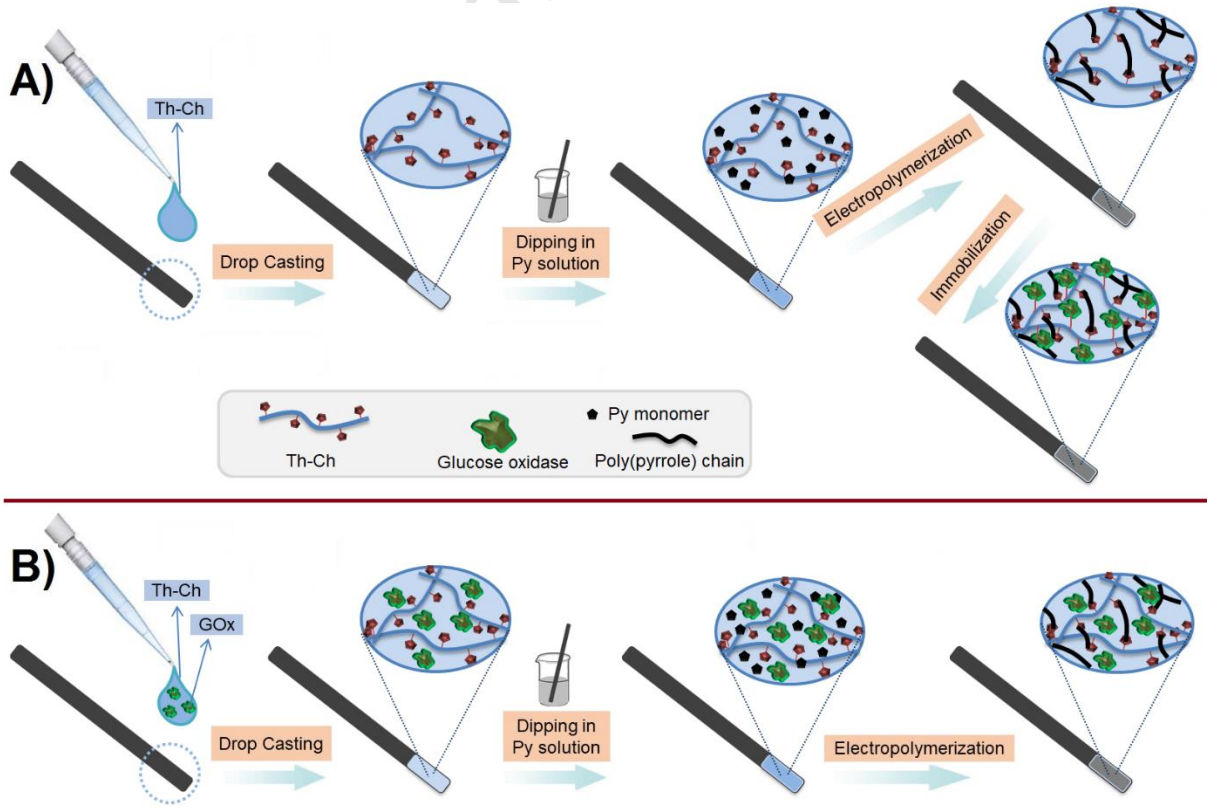

Figure 1. Schematic illustration of the fabrication process of glucose biosensor. **A)** Enzyme immobilization onto electropolymerized Ch-PTh-PPy, and **B)** entrapment of GOx into the Ch-PTh-PPy layer.

2.5. Cell culture and cytotoxicity testing

Adherent HaCaT (human keratinocyte, kindly provided by Prof. Ian Smyth, Monash University) cells were cultured in Dulbecco's Modified Eagle Medium (DMEM, Life Technologies) containing 4.5 g/L glucose, phenol red, 2 mM glutaMAX^{TM}, and supplemented with penicillin-streptomycin (100 units/mL and 100 µg/mL, respectively) and 10% fetal bovine serum (FBS, Scientifix). The cells were maintained in a humidified incubator at 37°C with 5% CO_2.

Prior to usage of any type of sensing electrode, heat sterilization was performed at 130^{o}C. Cytotoxicity testing of the Ch-PTh-PPy film and the PGE coated with Ch-PTh-PPy was undertaken using two experimental approaches; 1) a formazan based viability assay and 2) live/dead staining. The conditioned media test samples for the viability assay were prepared using the "extraction test" method as described by ISO 10993-5:2009(E) with minor modifications. Briefly, the electrode coated with Ch-PTh-PPy, or the Ch-PTh-PPy film (removed from PGE) was incubated in 500 µL of culture medium (24-well plate) for 48 h. Then the conditioned media samples were collected and filtered with a 0.2 µm pore size filter (Acrodisk®, Pall Corporation) in order to remove the remaining PGE particles after removing the Ch-PTh-PPy from the PGE surface. The viability of HaCaT cells cultured in the conditioned media was assessed using a tetrazolium compound [3-(4, 5-di methyl thiazol-2-yl)-5-(3-carboxymethoxy phenyl)-2-(4-sulfophenyl)-2H-tetrazolium, (MTS)] as per the manufacturer's instructions (Cell counting kit-8, Sigma Aldrich). Briefly, 5000 cells/well

were seeded in triplicate for each data point in a 96-well plate in DMEM culture media. 18 h after seeding, the media was replaced with neat (100%) conditioned media or conditioned media that had been diluted with fresh DMEM media (75%, 50%, 25%) and incubated for a further 24 h. 10 µL of the MTS assay reagent was added to each well, incubated for 1 h, and the absorbance at 490 nm was measured with a plate-reader (Multiskan™ FC Microplate Photometer, Thermofisher Scientific). The conditioned media with MTS in wells without cells was used as the "blank", and cells with normal DMEM media was used the "control". The % cell viability was calculated as follows $[(abs_{control} - abs_{sample}) / (abs_{control})] \times 100$.

Cytotoxicity testing via live/dead staining of HaCaT cells was performed by seeding $3x10^5$ cells/well (48-well plate) containing either Ch-PTh-PPy coated PGE or bare PGE (without Ch-PTh-PPy) in normal DMEM media. After 24 h incubation, the media was removed and the cells were incubated with 4 mM Calcein AM (Thermofisher Scientific) and 2 mM Propidium Iodide (Sigma) (diluted with sterile phosphate buffer saline (PBS)) for 30 min. The cells were imaged using a Nikon Eclipse Ts2 fluorescence microscope with Plan Fluor 4x/0.13 NA objective.

3. Results and Discussion

3.1. Characterizations of the Th-Ch

^{1}H NMR spectroscopy (Fig. 2A) confirmed the successful modification of Ch with 2-(thiophene-3-yl) acetic acid (Th-AA) due to the presence of Th NMR signals (δ 6.8 – 7.5 ppm). From the NMR spectrum, the conjugation efficiency was calculated to be around 8% by comparing the Th NMR signals with the NMR signal at 3.1 ppm that was attributed to unmodified Ch ($H2^{GlcN}$). Furthermore, ATR-FTIR (Fig. 2B) shows the appearance of a C=O amide stretch signal at 1646 cm^{-1} after Th conjugation. Thermogravimetric analysis showed a two-stage weight loss for both Ch and Th-Ch (see Fig. 2C). The first occurred in the range of

50 to 200°C, while the primary degradation started at 260°C and finished at around 500°C. Ch exhibited an earlier and higher weight loss in the first stage which was 13% that can be attributed to the stronger water adsorptive nature of Ch [31]. On the other hand, Th-Ch had a mild speed of decomposition during the temperature of 50 to 200°C showing the weight loss of 10%. This mild difference can be attributed to grafting of Ch with Th which could weaken hydrogen bonding [31, 32].

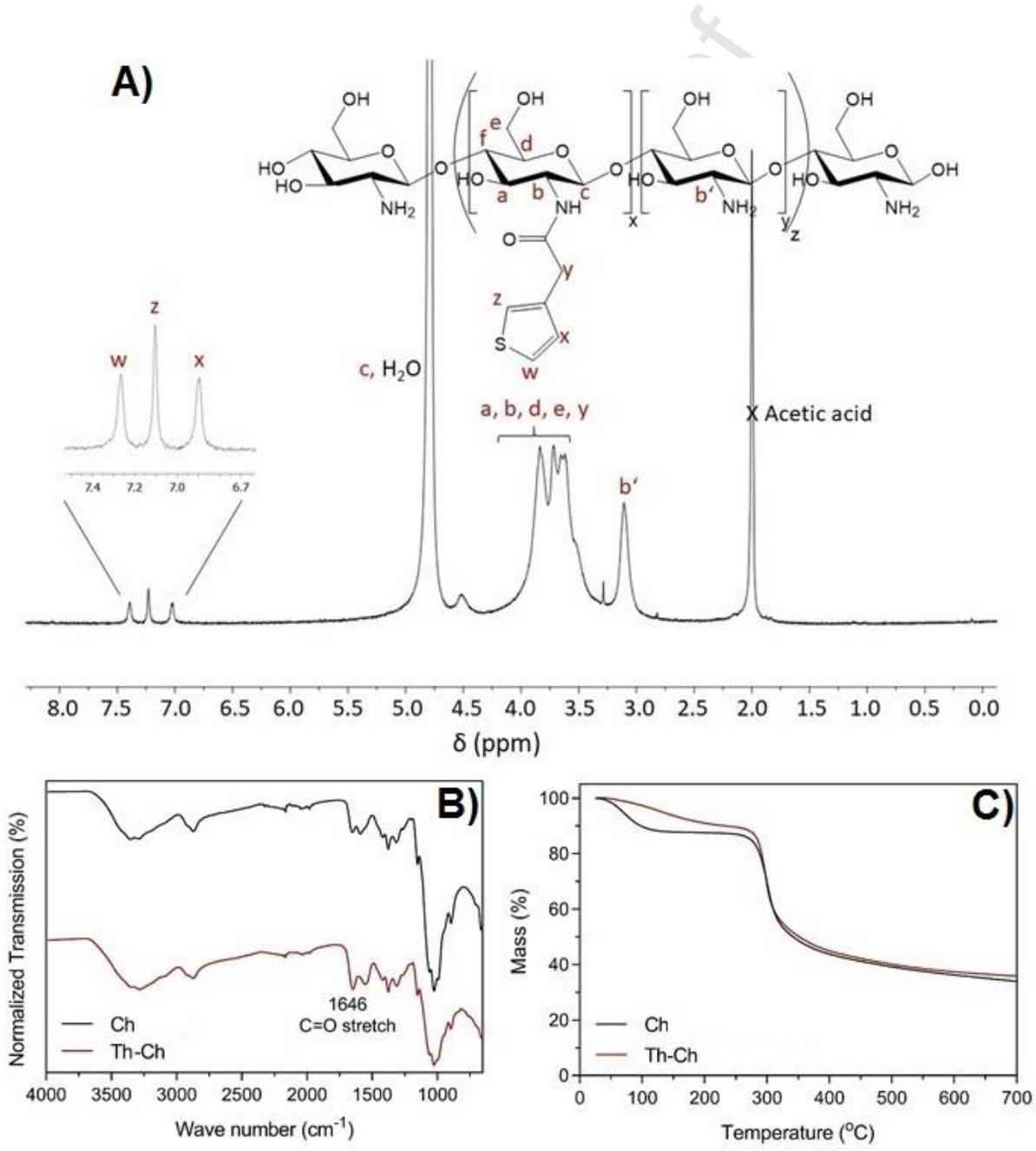

Figure 2. A) ^{1}H-NMR spectrum of Th-Ch in D_2O containing 5% CD_3COOD. **B)** FTIR-ATR spectra of Ch and Th-Ch. **C)** TGA thermogram of Ch and Th-Ch.

3.2. Optimization of electrocopolymerization conditions

Electropolymers of Py doped with p-toluenesulfonate composites are known to have excellent mechanical, physical, chemical properties and exhibit highly stable redox cycling [33]. Besides, doped PPy and PTh films show high electrical conductivity [34]. Electrochemical copolymerization of Py and Th has been accomplished by Naitoh et al. in 1986 [28] using 2,2'-thienylpyrrole (TP) as the starting monomer and by Kuwbata et al. in 1988 [35]. PPy and PTh both have good electrical conductivity however interestingly, electrocopolymerization of these tow homopolymers results in higher conductivity than for the respective homopolymers [28]. CV scans representing the reduction and oxidation current profile observed during the *in situ* electrocopolymerization of Th-Ch and Py are shown in Fig. S1. The increase in current intensity, as the number of cycle increases, is due to the formation of electrochemically active thin film, which increases the electrochemically active surface area on the electrode surface [36, 37]. The grafting of Th to Ch resulted in a more conductive film when compared to the one obtained with only Ch and Py (data not shown).

In order to obtain thin films with optimal electrochemical performance, several parameters of the preparation process were studied. Optimization was performed one step at a time starting with the amount of Th-Ch drop-casted on the electrode surface, proceeding with the concentration of the Py solution in which the electrode was incubated and the incubation time, and finally the number of CV cycles performed during the electrocopolymerization of the composite. Optimization experiments (see Fig. S2) were performed with CV in 0.5 mM $K_3[Fe(CN)_6]/K_4[Fe(CN)_6]$ (1:1 ratio) containing 0.1 M KCl solution in potential range of -0.1 V to 0.6 V at 100 mV/s scan rate. The parameter at which the highest oxidation and reduction

current intensity peaks were observed was selected as the optimum one. Results in Fig. S2A show that the amount of drop-casted Th-Ch which ranged from 2 to 16 µL, had no significant effect on electrode performance with not more than 10% variation in current response. On the other hand, Py concentration had a noteworthy effect on the electrode performance. As Py concentration increased from 0.1 to 1 M, a drastic increase in current response was seen. However, further increases in Py concentration resulted in a decrease of the response (Fig. S2B). The reason for this is that at lower monomer concentration the rate of conversion of monomer to polymer is high whereas at higher monomer concentration, the rate of conversion drops [38]. In addition, high Py concentrations can cause the formation of a passivating layer [39]. Incubation time of electrodes in Py solution was also studied. Fig. S2C shows the plot of current peak intensity obtained from CV data of electrocopolymerized films for different incubation times in Py solution ranging from 2 to 120 min. For the first 10 min, the current response drastically increased indicating successful absorption of Py solution by Th-Ch. Further increase in incubation time resulted in decrease of the response which is probably due to the delamination of Th-Ch film from electrode surface. The last parameter to be optimized was the number of cycles during electrocopolymerization. Increase in electrocopolymerization cycles up to 10 resulted in increase of current response (Fig. S2D), further increase in CV cycles decreased current response of the electrode, which can be due to the loss of the conductivity which can occur when the polymer is overoxidized [40]. In conclusion, for the fabrication of Th-Ch thin film with maximum electrochemical performance, 8 µL Th-Ch, 1 M Py solution with 10 min of incubation, and 10 CV cycles for *in situ* electrocopolymerization were used.

3.4. Morphological characterization

The surface topography was studied via AFM. Height images are represented in Fig. 3, where the same Z-range was applied for all images to aid visual comparison of surface

roughness. Drop-casting of either Ch (Fig. 3B) or Th-Ch (Fig. 3D) produced a smoother surface as compared to the bare PGE (Fig. 3A). Similar observations of smooth surfaces were obtained by means of SEM (see Fig. S2). Electropolymerization of Py in the presence of Ch (Ch-PPy) resulted in a change of morphology (Fig. 3C) as evidenced by the appearance of worm-like structures. Whereas for Ch-PTh-PPy, the roughness was similar to the PPy-only surface (see Fig. 3E and 3F) which shows that electropolymerization of Py absorbed by Th-Ch was successful. SEM images (see Fig. S3) reveal a smooth surface when Ch and Th-Ch were drop-casted and dried on the electrode surface. After *in situ* electrocopolymerization was performed, a change in the surface morphology with increased roughness and porosity of electropolymerized PPy in Ch and Th-Ch can be observed, indicating the successful electrodeposition of the polymer on the surface.

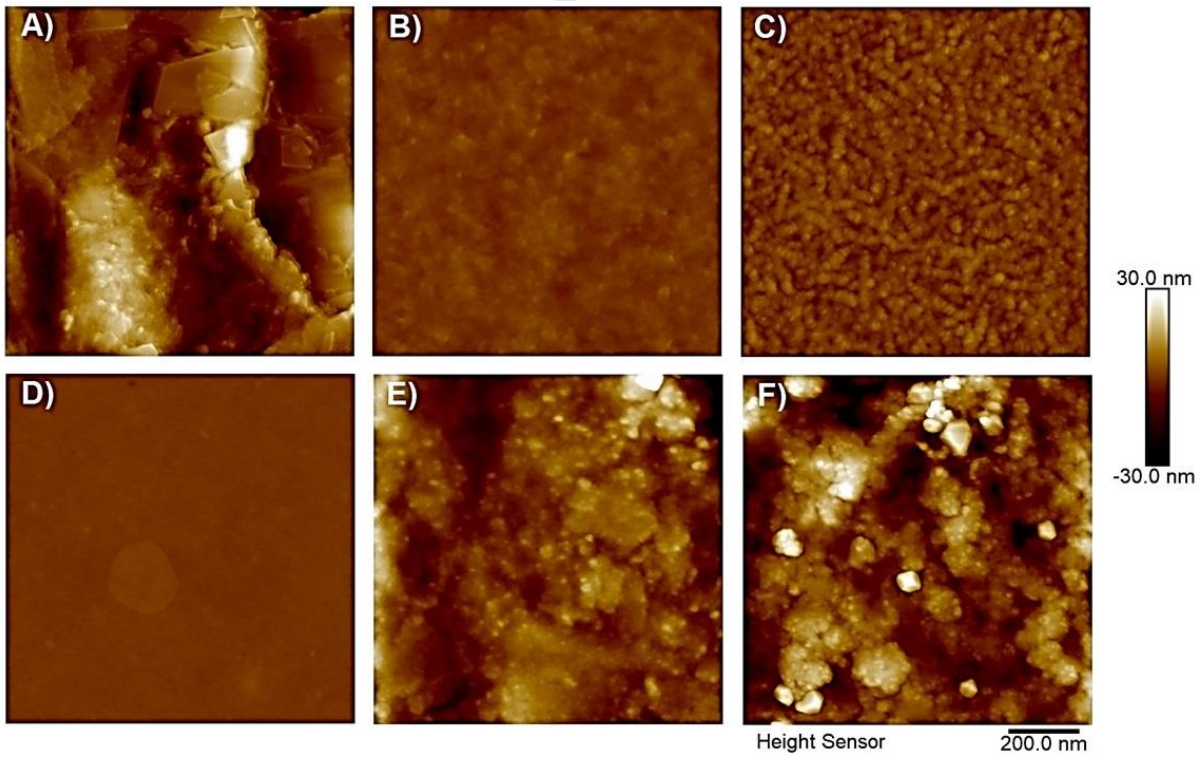

Figure 3. AFM height image of the **A)** PGE, **B)** drop-casted Ch, **C)** electropolymerized Ch-PPy, **D)** drop-casted Th-Ch, **E)** electropolymerized Ch-PTh-PPy, and **F)** electropolymerized PPy (scale bar: 200 nm; Z-range: 60 nm).

X-ray photoelectron spectroscopy (XPS, Fig. 4 and Table S1) was performed to determine the elemental composition for each sample surface. The Ch-coated sample clearly showed an increase in oxygen and nitrogen atomic concentrations as compared to the bare PGE, indicating successful coating. Further confirmation was obtained from high resolution C 1s spectra. For PGE, the C 1s spectrum was dominated by a single asymmetric peak representative of the carbon structure of graphite, with a shake-up feature at high binding energies (BEs) related to the pi-pi* transition. In the case of Ch coated on PGE, the spectral envelope is significantly different to that of PGE and consistent with Ch, while the shake-up feature of graphite is no longer observed, suggesting a relatively thick and pinhole-free coating, consistent with the observations from AFM. Interpreting the contributions to the Ch C 1s spectrum, two main peaks at 285.0 eV and 286.5 eV were assigned to aliphatic hydrocarbon and C-N/C-O groups, respectively, and a shoulder at 288.1 eV assigned to N-C=O/O-C-O groups. For the drop-casted Th-Ch sample, an additional increase in sulfur concentration was observed with a S/C value of 0.007 compared to 0.002 for Ch. The C 1s spectrum of Th-Ch was similar to Ch, albeit with a minor increase of intensity at lower BEs which is consistent with the addition of C-C and C-S bonds from the Th. From the S 2p spectrum (Fig. S4), the majority of the S was confirmed to be in the form of Th, with a smaller contribution to the spectrum at higher BEs associated with SOx; this contribution was also observed on other samples such as Ch. A control sample of PPy on PGE was analyzed, with a N/C value of 0.063 and a broadened main peak in the C 1s spectrum consistent with C-C and C-N from Py. For Ch-PPy small changes can be observe in the elemental composition and C 1s spectrum compared to Ch, whereas electropolymerization of Th-Ch with Py, Ch-

PTh-PPy, led to a significant reduction of oxygen and an increase in carbon concentration. As each Py unit consists of 4 carbon and 1 nitrogen atoms, this result provides evidence that a significant amount of Py has been incorporated only in the sample with Th present. The spectral envelope for Ch-PTh-PPy appears to have contributions from both PPy and Ch, with the main peak consistent with that observed for PPy, and two shoulders at higher BEs consistent with C-N/C-O groups and N-C=O/O-C-O groups observed for Ch.

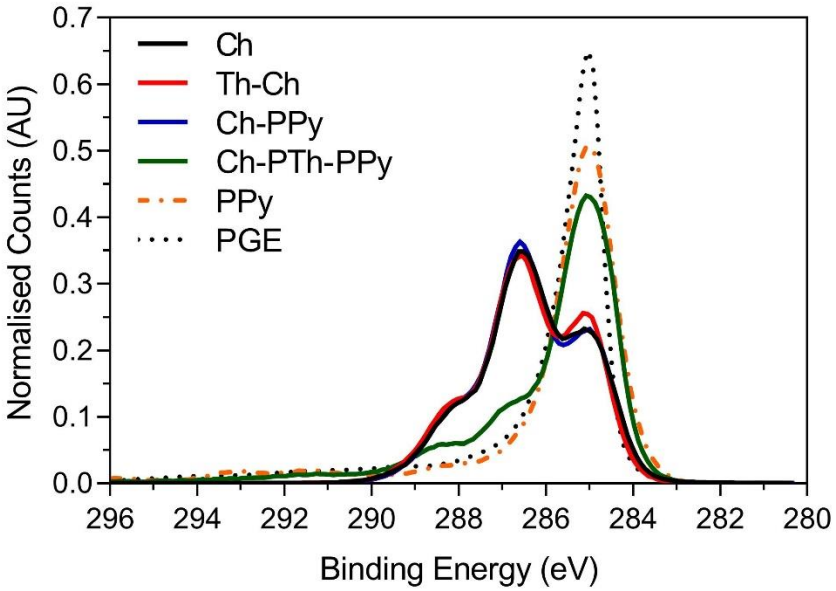

Figure 4. Representative high-resolution C 1s spectra from all samples detailed in Table S1. Each spectrum has been normalized to peak area and background subtracted (U 3 Tougaard), then overlaid to aid in the comparison of features in the spectral envelopes.

3.5. Cytotoxicity

To evaluate the cytotoxicity of the electrodes, MTS viability assay and live/dead staining were carried out. The colorimetric MTS assay relies on the metabolic activity of viable cells to reduce the tetrazolium substrate, and thereby produce a soluble colored formazan product, and the absorption of the final product is directly proportional to the metabolic rate of the viable cells. Here, human keratinocyte (HaCaT) cells were incubated for

24 h in various concentrations of conditioned media containing extracts (obtained by incubating the electrodes with media for 48 h) of the Ch-PTh-PPy-coated PGE, or the Ch-PTh-PPy film alone, followed by the evaluation of cell viability. Fig. 5A shows the cell viability relative to cells grown in medium without incubation with the electrodes (non-conditioned medium). Notably, cells cultured using conditioned medium of Ch-PTh-PPy-coated PGE exhibited a significant reduction in cell viability reaching 68% compared to controls. Dilution of this conditioned medium resulted in the increased viability suggesting that the Ch-PTh-PPy-coated PGE leached cytotoxic material into the media. Overall, cell viability was inversely proportional to the concentration (%, v/v) of the conditioned medium used to culture the cells. To investigate whether the cytotoxicity is caused by the Ch-PTh-PPy polymer alone, an MTS assay was conducted using conditioned medium of Ch-PTh-PPy film that had been manually removed from the PGE. Cell viability was unchanged compared to the control, regardless of the concentration (%v/v) of the conditioned medium used (no significant difference obtained with one way ANOVA, multiple comparison test, $p<0.05$). These studies indicate that the Ch-PTh-PPy-coated PGE exhibits cytotoxicity. Moreover, the source of cytotoxicity is likely the PGE and not the Ch-PTh-PPy polymer.

To further investigate the cytotoxicity of the Ch-PTh-PPy-coated PGE, live/dead staining of HaCaT cells cultured for 24 h in the presence or absence of the Ch-PTh-PPy-coated PGE was carried out. In contrast to MTS assays, live/dead staining of cells provides a quantitative measure of the proportion of viable and non-viable (dying) cells. The Calcein AM signal (green) identifies viable cells, and Propidium Iodide labels (red) the nucleus of cells with a compromised membrane integrity indicative of dead cells. As shown in the Fig. 5B & C, no significant change in the proportion of live/dead cells was observed between HaCaT cells co-cultured with the Ch-PTh-PPy-coated PGE (Fig. 5D), or bare PGE compared to control cells cultured without any type of electrode (comparison made with students t-test,

$p<0.01$). Therefore, live/dead staining indicates that the Ch-PTh-PPy-coated PGE is not cytotoxic.

The two approaches used here to assess the cytotoxicity of the Ch-PTh-PPy-coated PGE show an apparent discrepancy. The MTS assay indicates a significant ~32% reduction in the viability of cells cultured in Ch-PTh-PPy-coated PGE-conditioned media compared to control, in contrast to the live/dead staining which revealed no cytotoxic effect on cells co-cultured with the Ch-PTh-PPy-coated PGE. Notably, in this context the MTS assay does not account for the impact of a potential variation in the proliferation of cell populations grown under different conditions. A decrease in the proliferation rate of cells grown in conditioned *versus* non-conditioned media, may present an apparent decrease in cell viability in an MTS assay. The live/dead staining indicates that the PGE is not cytotoxic in terms of decreasing the number of living cells and increasing the number of dead cells (Fig. 5C). Although the number of stained cells are very close to each other (statistically insignificantly different), the results obtained with MTS assay indicate that the metabolic rate of cells exposed to conditioned media with polymer-coated PGE is lower than the control cells. Overall, in combination with a biocompatible electrode material such as gold, this material can make contact with the skin as a wearable sensing system.

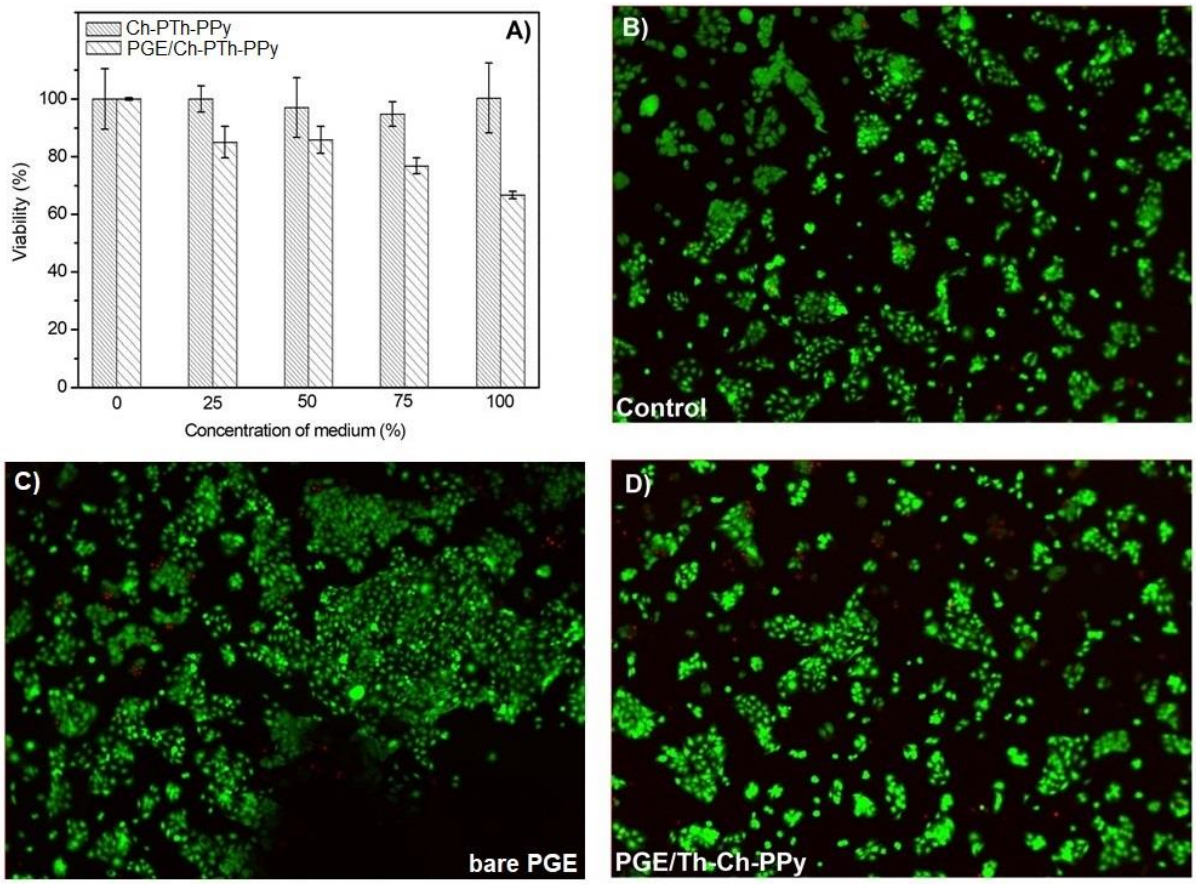

Figure 5. A) Cytotoxicity of Ch-PTh-PPy (densely striped bars) or PGE coated with Ch-PTh-PPy (striped bars) obtained with MTS assay (culture time 48h). The conditioned medium was used neat (100%) or at the indicated dilutions with non-conditioned medium shown *versus* the percentage of viable cells relative to the control cells (error bars represent standard deviation of data, n=3). HaCaT cells cultured in non-conditioned medium **B)** control, or with the **C)** bare PGE electrode, or with the **D)** PGE modified with Ch-PTh-PPy thin film, were stained with Calcein AM (green) and Propidium Iodide (red) to label viable and non-viable cells, respectively.

3.6. Electrochemical characterization

The electrochemical characterization of Th-Ch and Ch thin films was performed by means of CV and electrochemical impedance spectroscopy (EIS) in 0.5 mM $K_3[Fe(CN)_6]/K_4[Fe(CN)_6]$ (1:1 ratio) with 0.1 M KCl solution. Different configurations of

electrode modification strategies were studied by comparing the resulting working electrode`s electron transfer efficiency from the oxidation and reduction peak currents of CV scans, and the charge transfer resistivity obtained from the EIS scans. Comparison of CV and EIS plots was done by using bare PGE and modified PGE with drop-casted Ch and Th-Ch, respectively, as well as using similarly prepared Ch and Th-Ch electrodes on which *in situ* electropolymerization of Py was performed.

As illustrated in Fig. 6A, the oxidation-reduction current peaks are dependent on the modification process whilst a similar peak potential separation (ΔE_p) of approximately 120 mV was observed for all samples. In comparison with the bare electrode (Fig. 6A(a)), drop-casted Ch (Fig. 6A(b)) and Th-Ch (Fig. 6A(c)) showed a decreased redox peak intensity, which was expected due to the presence of nonconductive Ch. *In situ* electropolymerization of Py in the presence of Ch (Fig. 6A(d)) and electrocopolymerzation of Py and Th-Ch (Fig. 6A(e)) resulted in increase of the current peak intensities. The presence of Th in the Ch-PTh-PPy film resulted in higher electron transfer efficiency when compared to Ch-PPy. However, the electropolymerized Py alone (without Ch) demonstrated (Fig. 6A(f)) the highest intensity of oxidation-reduction current peaks, despite the reports that electrochemical copolymerization of Py and Th provides higher conductivity than Py and Th homopolymers alone [28, 35]. This is due to the lower concentration of Th (8%) present in the Th branched Ch polymer (see Fig. 2A) when compared to aforementioned reports. Although, the amount of grafted Th to Ch is small, it plays a crucial role by providing linking groups with Py during the electropolymerization.

These results were confirmed by performing EIS over a frequency range of 1 Hz to 10 kHz using similarly prepared electrodes. Fig. 6B shows Nyquist plot of EIS where charge transfer process at high frequency is semicircle portion of the plot and linear portion is a low frequency, which represents the diffusion process. The resistivity to the charge transfer

increased with the introduction of Ch (Fig. 6B(b)) with Rct of 742 Ω when compared to the bare electrode (Fig. 6A(a)) which has Rct value of 95 Ω. However, it decreased with the addition of Th to Ch to 610 Ω (Fig. 6B(c)). The surface coating with *in situ* electropolymerization of Py in the presence of Ch (Fig. 6B(d)) and electrocopolymerization of Py and Th-Ch (Fig. 6B(e)) resulted in electrodes with an even lower charge transfer resistivity of 440 Ω and 163 Ω, respectively. Finally, the conventional electropolymerization of Py on PGE had the lowest resistivity of 28 Ω, which is expected due to lacking Ch as the nonconductive material. These results are in good agreement with the results obtained using CV and show that the thin film obtained using newly synthesized Th-Ch polymer in combination with *in situ* electrocopolymerization of Py within the Th-Ch has a small electron transfer resistance, which is a highly favorable property in electrochemical biosensing applications.

Additionally, in order to obtain maximum response of Ch-PTh-PPy modified electrode, experiments were carried out to determine the optimum applied potential and the pH of buffer solution used for the electrochemical measurements (Fig. 6C and 6D). The current response of Ch-PTh-PPy electrode with GOx immobilized onto electrode surface (Fig.1A) to the same amount of added glucose was represented as a relative response (%) selecting the highest response as the maximum (100%). Fig. 6C shows the response at different applied potentials ranging from 0.4 V to 0.7 V, which increased as the applied potential increased, reaching its maximum at 0.6 V. Therefore, 0.6 V was selected as an optimum applied potential and it was used in further glucose sensing experiments. Fig. 6D represents the effect of pH change on the electrochemical response of glucose biosensor. Initially, an increase in pH resulted in a higher current response of the biosensor reaching its plateau at pH 7.4, while a further increase resulted in response decrement. As the maximum performance of the biosensor is in the physiological pH range, the engineered biosensor is

favorable for glucose sensing. Further, glucose sensing experiments were used to determine analytical performance of Ch-PTh-PPy thin film and to compare its performance with the Ch-PPy modified electrode.

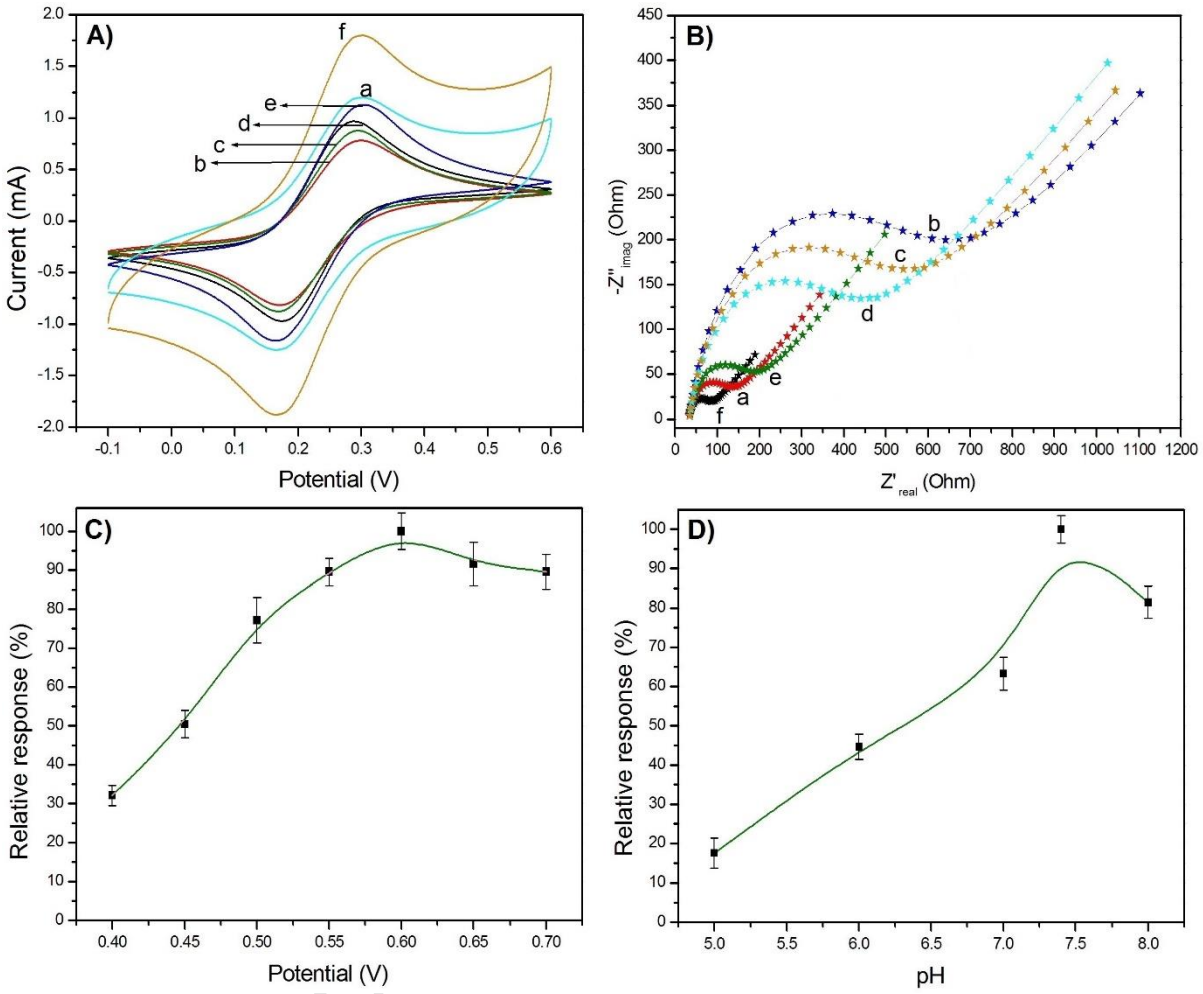

Figure 6. Comparison of a) bare PGE, drop-casted b) Ch and c) Th-Ch, and electropolymerized d) Ch-PPy, e) Ch-PTh-PPy and f) PPy with **A)** CV and **B)** EIS. Experimental results of the optimizations carried for the working **C)** potential and **D)** pH of Ch-PTh-PPy/GOx biosensor recorded in 0.1 M PBS (error bars: SD of n=3).

3.7. Glucose sensing performance

Amperometric glucose detection was performed for both Ch and Th-Ch-coated electrodes with different enzyme immobilization strategies: either surface modification of the

electrode through glutaraldehyde crosslinking after *in situ* electropolymerization of Ch or Th-Ch with Py (denoted as Ch-PPy/GOx and Ch-PTh-PPy/GOx, respectively), or entrapment of enzyme within the Ch or Th-Ch film followed by *in situ* electropolymerization of Py (denoted as Ch-GOx-PPy and Ch-PTh-GOx-PPy, respectively). Fig. 7A and 7B illustrate current *versus* time plots of *in situ* electropolymerized Ch and Th-Ch electrodes for the two immobilization strategies of GOx. The presence of Th significantly increased the current response regardless of the enzyme immobilization method used. The surface immobilization of GOx demonstrated the best analytical performance and had a response time of 3 s, a detection limit of 90 µM, a sensitivity of 10 µA/mM cm^{-2}, and a linear range of 1 to 8 mM of glucose. Moreover, Ch-PTh-PPy film provided approximately 40% higher sensitivity when compared to Ch-PPy composite. Normal blood glucose ranges from 3.5 to 5.5 mM [41], and in normal patients sweat glucose ranges from 10 µM to 0.2 mM [42] whereas in hyperglycemic patients sweat glucose can rise to 1 mM [43]. Therefore, it can be concluded that Ch-PTh-PPy/GOx can be utilized for the monitoring of both blood and sweat glucose levels.

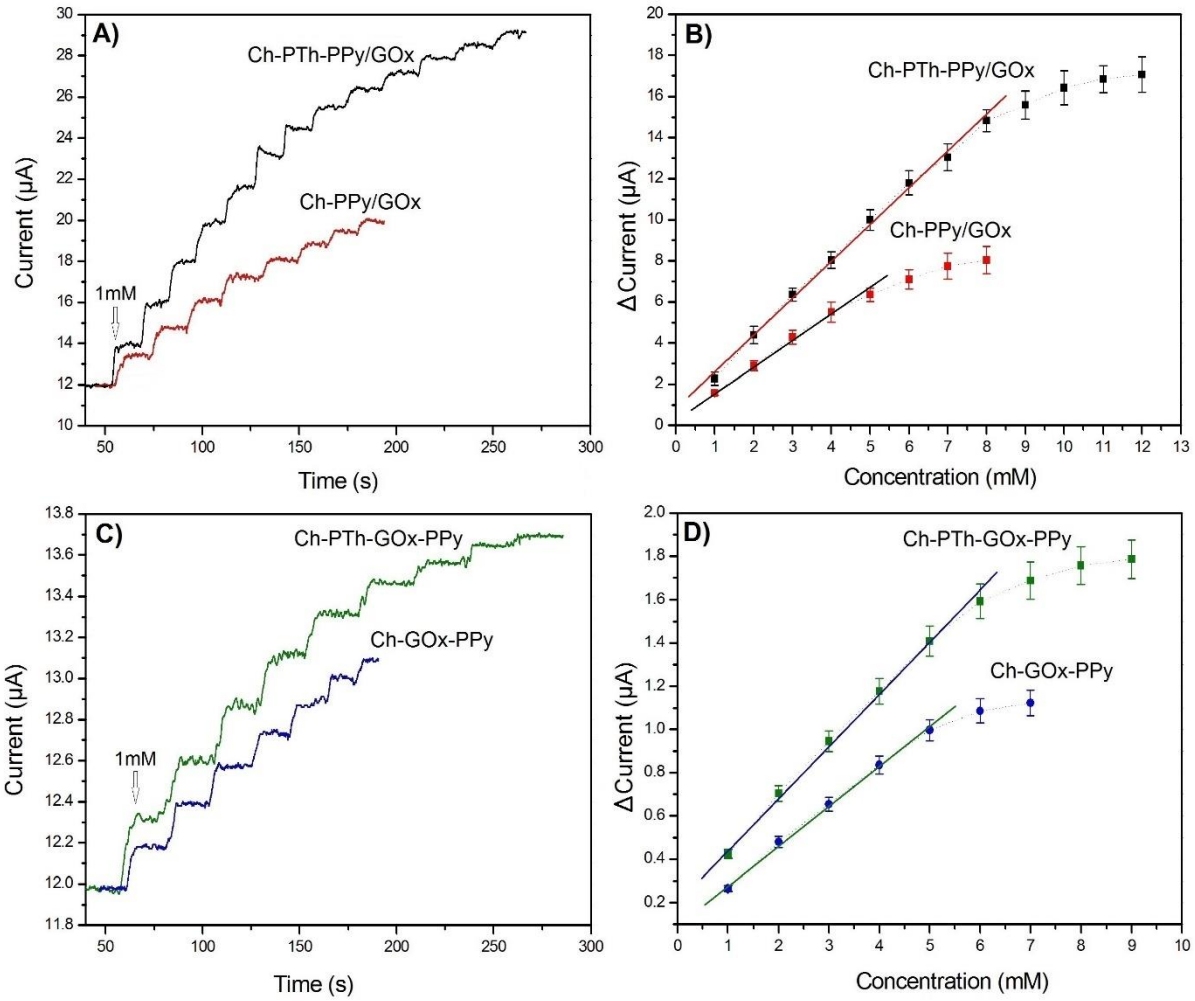

Figure 7. The amperometric response of Ch-PTh-PPy and Ch-PPy electrodes modified with GOx to 1 mM glucose additions in 0.1 M PBS pH 7.4. **A)** GOx immobilized on the electrode surface and **B)** calibration plots showing the concentration of detected glucose of Ch-PPy/GOx and Ch-PTh-PPy/GOx electrodes. **C)** GOx entrapped inside the electropolymerized films and **D)** calibration plots of Ch-GOx-PPy and Ch-PTh-GOx-PPy electrodes (error bars: SD of the data, n=3).

Table S2 shows a comparison of the analytical performances of all sensing electrodes prepared in this study. The entrapment of GOx within the Th-Ch followed by electrocopolymerization with Py resulted in poorer analytical performance when compared to the Ch-PTh-PPy/GOx electrode. This could be due to the limited substrate diffusion thorough the film and slight enzyme inactivation caused by the applied potential during

electrocopolymerization. A study of the operational stability showed that surface immobilization of GOx provided the sensing electrode with higher reusability (Fig. S5A). On the other hand, the entrapment of GOx scenario provided better long-term stability (Fig. S5B). To sum up, depending on the application needs, GOx could be either entrapped or later on immobilized onto the Ch-PTh-PPy thin film with this reported electrode fabrication methodology. GOx was used as the model enzyme to demonstrate the electrochemical performance of new Th-Ch polymer employed for the *in situ* copolymerization with Py. Notably, the analytical performance of the Ch-PTh-PPy electrode is competitive with previously reported biosensors based on Ch with PPy and different conductive nanomaterials such as Au nanoparticles (AuNPs), iron oxide nanoparticles (Fe_3O_4), and multiwalled carbon nanotubes (MWCNT) as shown in Table 1. However, further studies need to be performed to investigate the selectivity of the biosensor.

Table 1. Comparison of analytical performance of the Ch-PTh-PPy/GOx glucose biosensor with previously reported Ch based glucose biosensors.

Working electrode	Sensitivity	Detection Limit	Ref.
Ch- Fe_3O_4	9.3 μA/mM cm^{-2}	0.5 mM	[44]
Ch-Fc	0.798 nA/mM	0.565 mM	[45]
Ch-graphene-AuNPs	0.55 μA/mM	180 μM	[46]
Ch-N-graphene	10.5 μA/mM cm^{-2}	64 μM	[47]
Ch-MWCNT	8.017 μA/mM cm^{-2}	50 μM	[48]
GOx-Ch/PPy-AuNPs	0.58 μA/mM cm^{-2}	68 μM	[18]
PPy-Ch-Fe_3O_4	12 μA/mM cm^{-2}	234 μM	[19]
Ch-PTh-PPy/GOx	10 μA/mM cm^{-2}	90 μM	This work

4. Conclusion

A novel conductive thin film based on Th-grafted chitosan electrocopolymerized with Py was successfully prepared, characterized, and utilized in the fabrication of glucose biosensor. Th grafting was found to increase the electrical conductivity of the thin film and as

a consequence, decrease the charge transfer resistivity of the electrode surface when compared to Ch-PPy alone. The immobilization of enzyme after the *in situ* electrocopolymerization of Ch-PTh-PPy resulted in the highest analytical performance compared to the other studied biosensing electrode configurations. This novel Ch-PTh-PPy composite film is promising for enzymatic biosensing applications. Further studies will focus on the development of Ch-PTh-PPy nanocomposites using mediators, which are expected to decrease the working potential and increase selectivity with applications in wearable sweat biosensors.

Conflicts of Interest

The authors declare that they have no competing interests.

Acknowledgment

This work was performed in part at the Melbourne Centre for Nanofabrication (MCN) in the Victorian Node of the Australian National Fabrication Facility (ANFF).

References

[1] M. Mujtaba, R.E. Morsi, G. Kerch, M.Z. Elsabee, M. Kaya, J. Labidi, K.M. Khawar, Current advancements in chitosan-based film production for food technology; A review, International Journal of Biological Macromolecules 121 (2019) 889-904.

[2] S. Trombotto, C. Ladaviere, F. Delolme, A. Domard, Chemical preparation and structural characterization of a homogeneous series of chitin/chitosan oligomers, Biomacromolecules 9(7) (2008) 1731-8.

[3] W. Suginta, P. Khunkaewla, A. Schulte, Electrochemical Biosensor Applications of Polysaccharides Chitin and Chitosan, Chemical Reviews 113(7) (2013) 5458-5479.

[4] G. Ren, C. Clancy, T.M. Tamer, B. Schaller, G.M. Walker, M.N. Collins, Cinnamyl O-amine functionalized chitosan as a new excipient in direct compressed tablets with improved drug delivery, International Journal of Biological Macromolecules 141 (2019) 936-946

[5] T. Sarkar, H.B. Bohidar, P.R. Solanki, Carbon dots-modified chitosan based electrochemical biosensing platform for detection of vitamin D, International Journal of Biological Macromolecules 109 (2018) 687-697.

[6] X.-L. Luo, J.-J. Xu, J.-L. Wang, H.-Y. Chen, Electrochemically deposited nanocomposite of chitosan and carbon nanotubes for biosensor application, Chemical Communications (16) (2005) 2169-2171.

[7] X. Su, J. Ren, X. Meng, X. Ren, F. Tang, A novel platform for enhanced biosensing based on the synergy effects of electrospun polymer nanofibers and graphene oxides, Analyst 138(5) (2013) 1459-1466.

[8] M. Dervisevic, E. Dervisevic, E. Çevik, M. Şenel, Novel electrochemical xanthine biosensor based on chitosan–polypyrrole–gold nanoparticles hybrid bio-nanocomposite platform, Journal of Food and Drug Analysis 25(3) (2017) 510-519.

[9] Y. Shu, J. Chen, Q. Xu, Z. Wei, F. Liu, R. Lu, S. Xu, X. Hu, MoS2 nanosheet–Au nanorod hybrids for highly sensitive amperometric detection of H2O2 in living cells, Journal of Materials Chemistry B 5(7) (2017) 1446-1453.

[10] L. Yu, Q. Zhang, D. Jin, Q. Xu, X. Hu, A promising voltammetric biosensor based on glutamate dehydrogenase/Fe3O4/graphene/chitosan nanobiocomposite for sensitive ammonium determination in PM2.5, Talanta 197 (2019) 622-630.

[11] P. Naderi Asrami, S.A. Mozaffari, M. Saber Tehrani, P. Aberoomand Azar, A novel impedimetric glucose biosensor based on immobilized glucose oxidase on a CuO-Chitosan nanobiocomposite modified FTO electrode, International Journal of Biological Macromolecules 118 (2018) 649-660.

[12] L. Luo, L. Zhu, Y. Xu, L. Shen, X. Wang, Y. Ding, Q. Li, D. Deng, Hydrogen peroxide biosensor based on horseradish peroxidase immobilized on chitosan-wrapped NiFe2O4 nanoparticles, Microchimica Acta 174(1) (2011) 55-61.

[13] A.M. Santos, A. Wong, F.H. Cincotto, F.C. Moraes, O. Fatibello-Filho, Square-wave adsorptive anodic stripping voltammetric determination of norfloxacin using a glassy carbon electrode modified with carbon black and CdTe quantum dots in a chitosan film, Microchimica Acta 186(3) (2019) 148.

[14] Y. Wang, S. Wang, L. Tao, Q. Min, J. Xiang, Q. Wang, J. Xie, Y. Yue, S. Wu, X. Li, H. Ding, A disposable electrochemical sensor for simultaneous determination of norepinephrine and serotonin in rat cerebrospinal fluid based on MWNTs-ZnO/chitosan composites modified screen-printed electrode, Biosensors and Bioelectronics 65 (2015) 31-38.

[15] Y. Jiang, J. Wu, Recent development in chitosan nanocomposites for surface-based biosensor applications, ELECTROPHORESIS 40(16-17) (2019) 2084-2097.

[16] Z. Geng, X. Wang, X. Guo, Z. Zhang, Y. Chen, Y. Wang, Electrodeposition of chitosan based on coordination with metal ions in situ-generated by electrochemical oxidation, Journal of Materials Chemistry B 4(19) (2016) 3331-3338.

[17] Y.-x. Zhao, K.-f. Ren, Y.-x. Sun, Z.-j. Li, J. Ji, Thin electroconductive hydrogel films by in situ electropolymerization of pyrrole within polyelectrolyte multilayers, RSC Advances 4(47) (2014) 24511-24517.

[18] M. Şenel, Simple method for preparing glucose biosensor based on in-situ polypyrrole cross-linked chitosan/glucose oxidase/gold bionanocomposite film, Materials Science and Engineering: C 48 (2015) 287-293.

[19] A.M.A. Abdul Amir Al-Mokaram, R. Yahya, M.M. Abdi, H.N. Muhammad Ekramul Mahmud, One-step electrochemical deposition of Polypyrrole–Chitosan–Iron oxide

nanocomposite films for non-enzymatic glucose biosensor, Materials Letters 183 (2016) 90-93.

[20] Y. Liu, X. Feng, J. Shen, J.-J. Zhu, W. Hou, Fabrication of a Novel Glucose Biosensor Based on a Highly Electroactive Polystyrene/Polyaniline/Au Nanocomposite, The Journal of Physical Chemistry B 112(30) (2008) 9237-9242.

[21] Y. Li, S. Yin, Y. Lu, H. Zhou, H. Jiang, N. Niu, H. Huang, L. Zhang, K.K.-W. Lo, C. Yu, Choline sensing based on in situ polymerization of aniline on the surface of upconverting nanoparticles, Journal of Materials Chemistry B 5(38) (2017) 7861-7865.

[22] M. Şenel, C. Nergiz, M. Dervisevic, E. Çevik, Development of Amperometric Glucose Biosensor Based on Reconstitution of Glucose Oxidase on Polymeric 3-Aminophenyl Boronic Acid Monolayer, Electroanalysis 25(5) (2013) 1194-1200.

[23] M. Dervisevic, M. Senel, E. Cevik, Novel impedimetric dopamine biosensor based on boronic acid functional polythiophene modified electrodes, Materials Science and Engineering: C 72 (2017) 641-649.

[24] M. Dervisevic, M. Senel, T. Sagir, S. Isik, Highly sensitive detection of cancer cells with an electrochemical cytosensor based on boronic acid functional polythiophene, Biosensors and Bioelectronics 90 (2017) 6-12.

[25] S. Nandini, S. Nalini, J. Sanetuntikul, S. Shanmugam, P. Niranjana, J.S. Melo, G.S. Suresh, Development of a simple bioelectrode for the electrochemical detection of hydrogen peroxide using Pichia pastoris catalase immobilized on gold nanoparticle nanotubes and polythiophene hybrid, Analyst 139(22) (2014) 5800-5812.

[26] P. Liu, P. Du, J. Guo, X. Wu, J. Qiu, Facile mass production of semi-conductive polypyrrole/polystyrene composite with enhanced mechanical strength via in-situ bulk polymerization, Materials Letters 139 (2015) 191-193.

[27] D. Ye, L. Luo, Y. Ding, Q. Chen, X. Liu, A novel nitrite sensor based on graphene/polypyrrole/chitosan nanocomposite modified glassy carbon electrode, Analyst 136(21) (2011) 4563-9.

[28] S. Naitoh, K. Sanui, N. Ogata, Electrochemical synthesis of a copolymer of thiophene and pyrrole: poly(thienylpyrrole), Journal of the Chemical Society, Chemical Communications (17) (1986) 1348-1350.

[29] X. Li, M. Lu, H. Li, Electrochemical copolymerization of pyrrole and thiophene nanofibrils using template-synthesis method, Journal of Applied Polymer Science 86(10) (2002) 2403-2407.

[30] S. Khademi, B. Pourabbas, K. Foroutani, Synthesis and characterization of poly(thiophene-co-pyrrole) conducting copolymer nanoparticles via chemical oxidative polymerization, Polymer Bulletin 75(9) (2018) 4291-4309.

[31] A.H. Gedam, R.S. Dongre, Adsorption characterization of Pb(ii) ions onto iodate doped chitosan composite: equilibrium and kinetic studies, RSC Advances 5(67) (2015) 54188-54201.

[32] G. Ma, D. Yang, J.F. Kennedy, J. Nie, Synthesize and characterization of organic-soluble acylated chitosan, Carbohydrate Polymers 75(3) (2009) 390-394.

[33] C. Jin, F. Yang, W. Yang, Electropolymerization and ion exchange properties of a polypyrrole film doped by para-toluene sulfonate, Journal of Applied Polymer Science 101(4) (2006) 2518-2522.

[34] E. Ando, S. Onodera, M. Iino, O. Ito, Electric conductivity changes of polypyrrole and polythiophene films with heat-treatment, Carbon 39(1) (2001) 101-108.

[35] S. Kuwabata, S. Ito, H. Yoneyama, Copolymerization of Pyrrole and Thiophene by Electrochemical Oxidation and Electrochemical Behavior of the Resulting Copolymers, Journal of The Electrochemical Society 135(7) (1988) 1691-1695.

[36] N. Guven, P. Camurlu, Electrosyntheses of anthracene clicked poly(thienylpyrrole)s and investigation of their electrochromic properties, Polymer 73 (2015) 122-130.

[37] E. Cordruwisch, G.S. Popkirov, E. Türk, J. Theiner, G.E. Nauer, Redox behaviour of thin films of poly(thienylpyrrole) characterized by in situ measurement of high frequency resistance, Electrochimica Acta 41(7) (1996) 1369-1374.

[38] S. Maiti, D. Das, K. Sen, Electrochemical Polymerization of Pyrrole: Key Process Control Parameters, Journal of The Electrochemical Society 159(9) (2012) E154-E158.

[39] M. Zhou, M. Pagels, B. Geschke, J. Heinze, Electropolymerization of Pyrrole and Electrochemical Study of Polypyrrole. 5. Controlled Electrochemical Synthesis and Solid-State Transition of Well-Defined Polypyrrole Variants, The Journal of Physical Chemistry B 106(39) (2002) 10065-10073.

[40] B. Schweiger, J. Kim, Y.J. Kim, M. Ulbricht, Electropolymerized molecularly imprinted polypyrrole film for sensing of clofibric acid, Sensors (Basel, Switzerland) 15(3) (2015) 4870-89.

[41] M. Guemes, S.A. Rahman, K. Hussain, What is a normal blood glucose?, Archives of disease in childhood 101(6) (2016) 569-574.

[42] M. Bariya, H.Y.Y. Nyein, A. Javey, Wearable sweat sensors, Nature Electronics 1(3) (2018) 160-171.

[43] H. Lee, C. Song, Y.S. Hong, M.S. Kim, H.R. Cho, T. Kang, K. Shin, S.H. Choi, T. Hyeon, D.-H. Kim, Wearable/disposable sweat-based glucose monitoring device with multistage transdermal drug delivery module, Science Advances 3(3) (2017) e1601314.

[44] A. Kaushik, R. Khan, P.R. Solanki, P. Pandey, J. Alam, S. Ahmad, B.D. Malhotra, Iron oxide nanoparticles–chitosan composite based glucose biosensor, Biosensors and Bioelectronics 24(4) (2008) 676-683.

[45] Ö. Yılmaz, D.O. Demirkol, S. Gülcemal, A. Kılınç, S. Timur, B. Çetinkaya, Chitosan–ferrocene film as a platform for flow injection analysis applications of glucose oxidase and Gluconobacter oxydans biosensors, Colloids and Surfaces B: Biointerfaces 100 (2012) 62-68.

[46] C. Shan, H. Yang, D. Han, Q. Zhang, A. Ivaska, L. Niu, Graphene/AuNPs/chitosan nanocomposites film for glucose biosensing, Biosensors and Bioelectronics 25(5) (2010) 1070-1074.

[47] M.M. Barsan, M. David, M. Florescu, L. Ţugulea, C.M.A. Brett, A new self-assembled layer-by-layer glucose biosensor based on chitosan biopolymer entrapped enzyme with nitrogen doped graphene, Bioelectrochemistry 99 (2014) 46-52.

[48] Y. Zou, C. Xiang, L. Sun, F. Xu, Amperometric glucose biosensor prepared with biocompatible material and carbon nanotube by layer-by-layer self-assembly technique, Electrochimica Acta 53(12) (2008) 4089-4095.

Author Statement

Mehmet Senel: Conceptualization, Methodology, Validation, Investigation, Resources, Writing - Original Draft, Supervison, **Muamer Dervisevic:** Methodology, Validation, Investigation, Writing - Review & Editing, **Lars Esser:** Methodology, Validation, Investigation, **Esma Dervisevic:** Methodology, Validation, Investigation, **Jennifer Dyson:** Methodology, Writing - Review & Editing, Supervision, **Christopher D. Easton:** Methodology, Supervision, **Victor J. Cadarso:** Resources, Writing - Review & Editing, **Nicolas H. Voelcker:** Resources, Writing - Review & Editing, Supervision

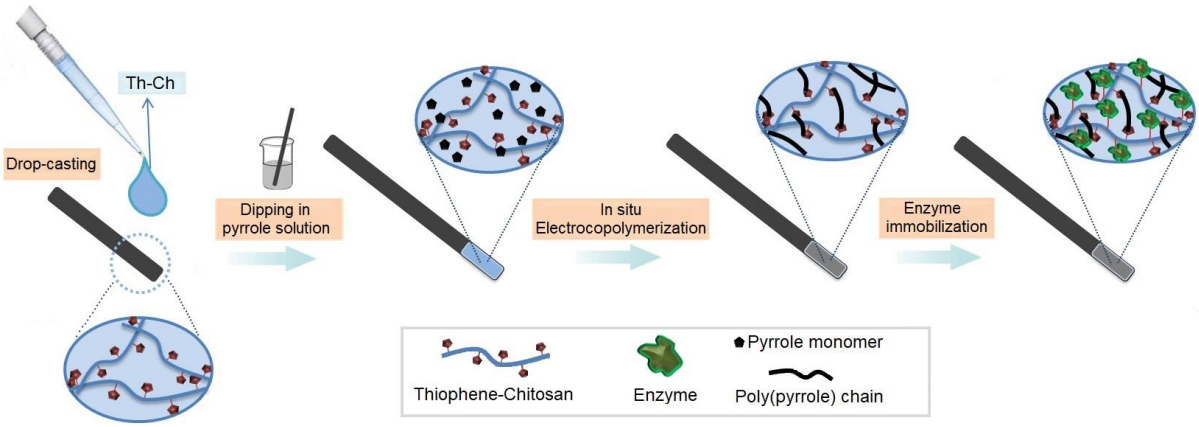

Graphical abstract